ORIGINAL PAPER

Investigation of Ewekoro Formation using 2D electrical resistivity tomography—a case study from Nigeria

Elijah Adebowale Ayolabi[1,2] · Rita Chinnoye Michael[3]

Abstract

Geophysical investigation of the Ewekoro Formation around Ibese mines, Ogun state, Nigeria, was carried out by deploying the 2D electrical resistivity tomography (ERT) method for characterizing the sub-surface stratigraphy sequence and cavitation zones. Eight 2D profiles were established, and electrical resistivity data were acquired using dipole–dipole and pole-dipole arrays. A maximum of four geoelectric layers/strata were mapped. The uppermost beds are composed mainly of clay and in some cases sand and shale at depths ranging from 0 to 7.5 m and resistivity values between 1.0 and 5550 Ωm. The second layer is composed of shale and, in some cases, limestone with a resistivity range of 1.0–13,000 Ωm and depth range of 1.0–36 m. The high resistivity (1000 to 13,000 Ωm) in this band was interpreted to be limestone. The third geoelectric component was predominantly made up of limestone at depths 3–39.4 m and resistivity of 80–13,000 Ωm. The fourth layer is composed of marl occurring from 17 to 57 m and resistivity of 10.7–400 Ωm. The overburden was evaluated to be between 2.0 and 14.5-m thick while the limestone thickness was found to be between 5.9 and 31.45 m. This research established the presence of cavity structures with a resistivity range of 1.0–50 Ωm which could help guide mining engineers in preventing geohazard and flooding during the mining operation.

Keywords Limestone · Resistivity · Layer · Depth · Cavities · Geo-electric · Overburden

Introduction

The Ewekoro Formation houses one of Nigeria's major limestone deposits, which serves as raw material for cement manufacturing plants in the southwestern part of Nigeria. Ewekoro limestone is sometimes overlaid by hard shale and underlined by calcareous sandstone. Limestone is pale white to buff-colored, medium to coarse-grained. Occasionally, thin bands of siliceous limestone are also observed. Limestone is an example of a sedimentary rock mainly of calcite ($CaCO_3$) mineral, formed as a result of either biological or chemical processes (Serra 2006). Nigeria has vast limestone resources in the country (Felix and Yomi 2013).

Mineral deposits have been successfully identified and delineated by geophysical methods and have extremely reduced ambiguities in mineral exploitation (Haile and Atsbaha 2014). The electrical resistivity method of geophysical prospecting is an economical non-invasive method, that can provide 2D or 3D models of the subsurface (Lara and Giovanni 2019; Hussain et al. 2020; Gobashy et al. 2021; Ameloko and Ayolabi 2020; Ameloko et al. 2020; Obihan et al. 2021). This provides a key advantage over the intrusive sampling method, providing information only at isolated locations (Ayolabi et al. 2009).

Mapping of the shallow-weathered zone and cavities employing geophysical techniques has gained

✉ Rita Chinnoye Michael
okwuigalarita@yahoo.com

1 Department of Geosciences, Mountain Top University, Ibafo, Ogun State, Nigeria

2 Department of Geosciences, University of Lagos, Akoka Yaba, Lagos State, Nigeria

3 Department of Environmental Management and Toxicology, Federal University of Agriculture, Abeokuta, Ogun State, Nigeria

wide interest in the past few decades (Sum et al. 1996; Mohamed and Fouzan 2013). The occurrence of natural cavities and voids in the limestone can cause serious problems for miners, environmental management, and civil engineering. One of the major factors affecting limestone is porosity, which is the volume of pores to the volume of bulk rock (limestone) and determines the amount of moisture contained in it (Rita and Adedeji 2021). Rocks contain inter-grain spaces sometimes occupied with fluid or solution cavities (Oluwaseun et al. 2012; Golian et al. 2020), thereby decreasing the electric resistance of that rock. Hence, electrical resistivity tomography can delineate limestone as well as overburden thickness provided sufficient contrast exists between the overburden (Ammar and Kamal 2018) and the limestone.

Electrical resistivity imaging is one of the most frequently utilized geophysical methods in mapping weathered zones and cavities. It offers a cost-effective and quick exploration of the near subsurface with acceptable results. Therefore, the objective of the study is to map the subsurface geology of the concession area from their electrical conductivity distribution, as a means of defining the main lithologic units, the geometry of the limestone bands, and possible cavitation zones.

Geomorphology of Study Area

The study area is located in Yewa Local Government Area, Ogun State in Nigeria. It has geographical coordinates of latitude 773,212.93 mN and 772,566.58 mN and longitude 503928.1 mE and 504663.04 mE (Fig. 1). The site is generally flat with minimum and maximum elevations of 38.12 m and 57.59 m, respectively, above Lagos Datum (mean sea level). It has an almost flat topography with localized low-lying areas. These low-lying areas are generally waterlogged during rainy season because of a poor drainage system and flat ground. The highest elevation is towards the southeastern part, about 57.59 m above sea level (Fig. 1), generally sloping towards NW-, and the drainage joins the river Iniya which is flowing towards NW to join the major river Yewa. A seasonal stream running NW-SW was observed to drain the area.

Ibese is located at the southern edge of the Ewekoro depression in Dahomey basin and is overlooked by the escarpment capped by the Ilaro Formation (Fig. 2), which forms a conspicuous feature (Ozebo et al. 2008). Limestone deposit of economic interest is the thick limestone body near the base of the Ewekoro Formation observed at Shagamu, Ewekoro town, and the North of Ibese, which occurs at varying depths. Ewekoro Formation consists of algae limestone
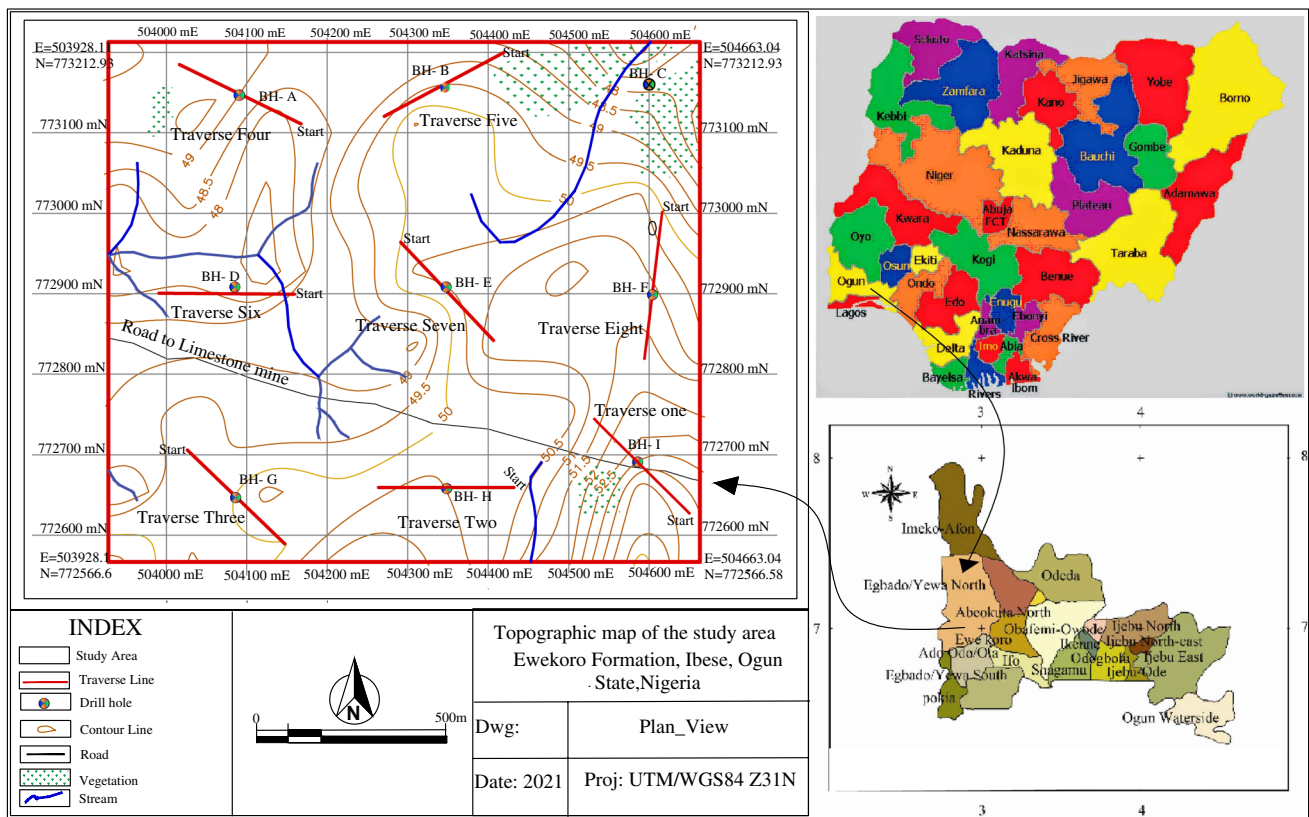

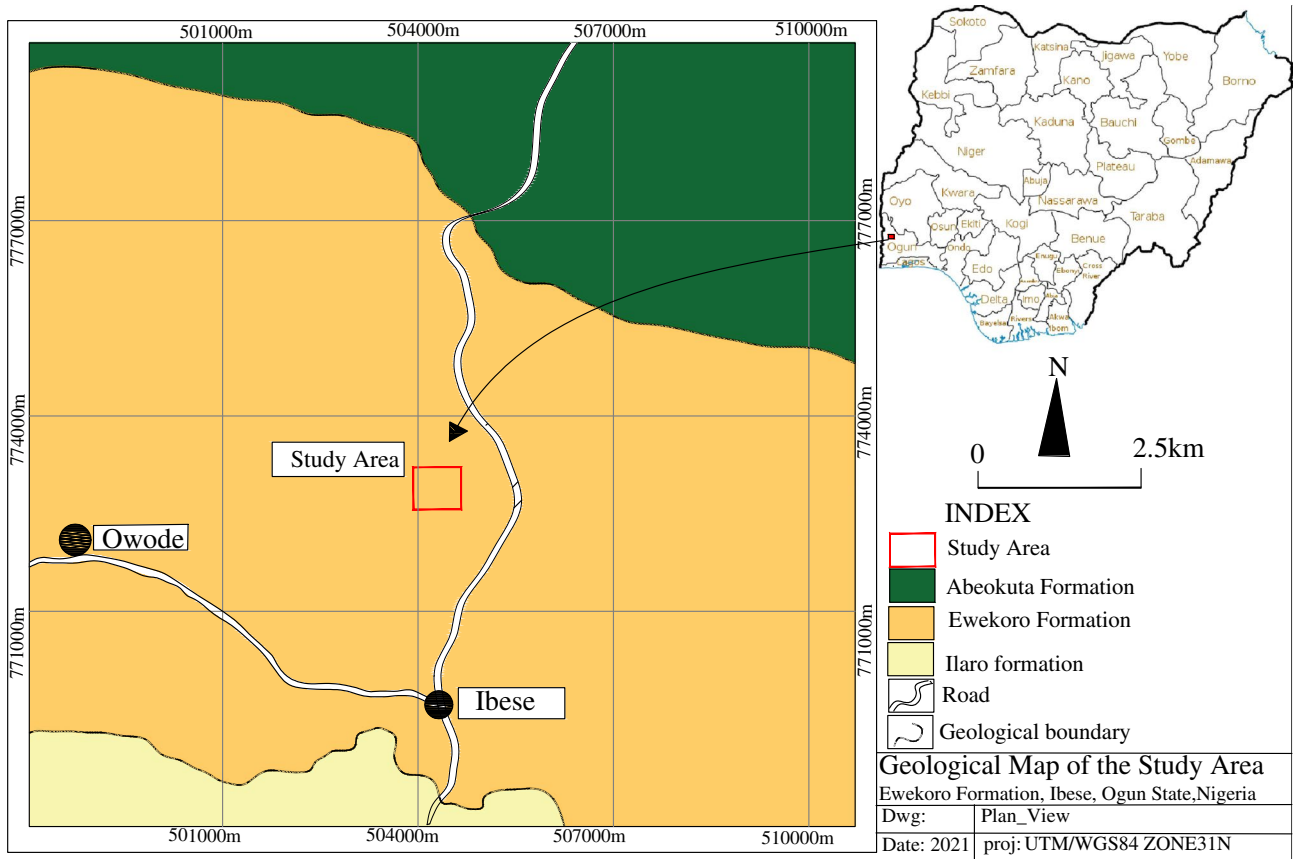**Fig. 1** Topography of the study area

Fig. 2 Stratigraphic of Dahomey basin (geological survey of Nigeria 1963)

of varying thickness, overlain by finely laminated black and gray shales interbedded with marl. The grayish shales at the top of the sequence grade into thick reddish clay and sand. These have been tentatively referred to as Akinbo and Oshosun Formations, respectively (Ozebo et al. 2008).

This limestone deposit is free from any major structural disturbances. The general strike of the limestone is NW to SE and dipping towards the South; hence, the thickness of the overlain shale increases towards the south. Since it is a shallow marine deposit, many karst topographic features and cavities have been observed in the limestone zone.

Previous field studies and available drill logs confirmed that the sediments in Ibese consist essentially of Oshsun Formation—lateritic clay and conglomerate, sandstone, and the Akinbo Formation is dark gray/black shales with discontinuous limestone and marl bands of the Ewekoro Formation.

Methodology

The electrical resistivity technique was selected as a suitable approach in delineating the geology due to the expected contrast in the electrical resistivity representation of the subsurface geology. The 2D ERT data used for the investigation of the Ewekoro Formation was acquired via the Super Sting R8 Earth Resistivity/IP meter (automated multi-electrode system). The instrument used 84 electrodes and was deployed alongside an electrode selector and other accessories for the study. Eight profiles, at 2-m inter-electrode spacing, were occupied in the entire study area using the dipole–dipole and pole-dipole configuration (Fig. 3). The choice of these electrode spreads lies in their high sensitivity to horizontal changes in resistivity and high signal strength, respectively (Loke and Barker 1996).

The 2D data obtained from the survey were processed and inverted using the Earth Imager inversion algorithm (AGI 2003), to produce the resistivity models. The apparent resistivity was determined via a forward modeling subroutine, with the inversion scheme performed by the software by means of the least-square optimization routine (Loke 2003). The computer program determines the resistivity of a series of rectangular cells so that the measured values agreed with the calculated apparent resistivity values.

The processed data were correlated with borehole logs and interpreted, thereby resulting in the identification of the various lithologies and the limestone deposits in the study location. The variation in resistivity and thickness

Fig. 3 Dipole–dipole electrode array with apparent resistivity and pole-dipole electrode array with apparent resistivity (after Morrison and Gasperikova 2012)
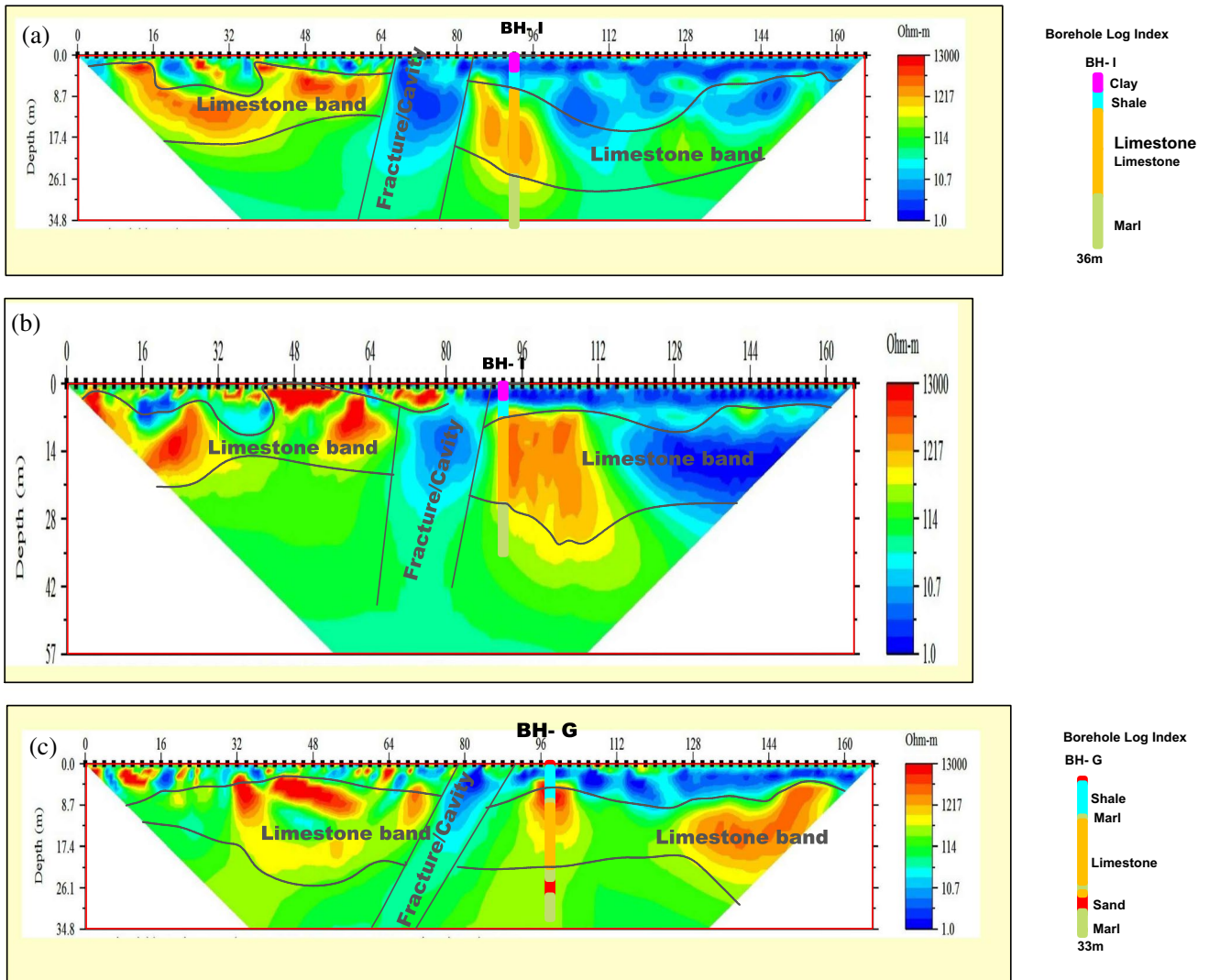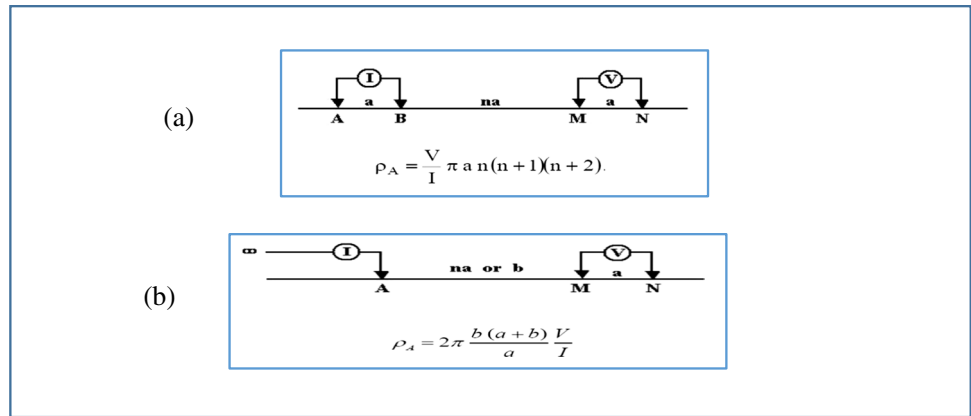
(a)

$$\rho_A = \frac{V}{I} \pi\, a\, n(n+1)(n+2).$$

(b)

$$\rho_A = 2\pi\, \frac{b\,(a+b)}{a}\, \frac{V}{I}$$

Fig. 4 2D ERT along traverse one and three. (**a**) dipole-dipole array along traverse one. (**b**) pole-dipole array along traverse one. (**c**) dipole-dipole array along traverse three

Table 1 Summary of borehole the detail versus geo-electric characterization

S/No	Bore hole ID	Borehole depth (m)	From (m)	To (m)	Lithology	Geo-electric depth probed@ borehole point (m)	
1	BH- I	36.0	0.0	3.0	Clay	0.0	3.0
			3.0	7.5	Shale	3.0	7.0
			7.5	25.5	Limestone	7.0	28.0
			25.5	36.0	Marl	28.0	57.0
2	BH- H	37.0	0.0	1.0	Clay	0.0	1.5
			1.0	1.5	Sand		
			1.5	9.5	Shale	1.5	6.0
			9.5	22.5	Limestone	6.0	26.2
			22.5	25.0	Marl	26.2	57.0
			25.0	27.0	Limestone		
			27.0	28.0	Marl		
			28.0	29.5	Sand		
			29.5	37.0	Marl		
3	BH- G	33.0	0.0	1.0	Sand	0.0	1.0
			1.0	8.0	Shale	1.0	5.2
			8.0	9.0	Marl	5.2	22.0
			9.0	22.0	Limestone		
			22.0	24.0	Marl	22.0	34.8
			24.0	24.5	Limestone		
			24.5	28.0	Sand		
			28.0	33.0	Marl		
4	BH- A	28.0	0.0	1.0	Clay	2.4 m exca-vated	
			1.0	5.5	Shale	2.4	5.0
			5.5	26.0	Limestone	5.0	27.5
			26.0	27.0	Marl	27.5	57.0
			27.0	27.5	Limestone		
			27.5	28.0	Marl		
5	BH- B	28.0	0.0	3.0	Clay	0.0	3.5
			3.0	12.0	Limestone	3.5	12.0
			12.0	28.0	Marl	12.0	53.0
6	BH- D	30.0	0.0	1.5	Sand	0.0	0.5
			1.5	6.0	Shale	0.5	4.5
			6.0	22.5	Limestone	4.5	21.5
			22.5	30.0	Marl	21.5	57.0
7	BH- E	36.0	0.0	1.0	Clay	0.0	0.5
			1.0	6.0	Shale	0.5	4.8
			6.0	27.0	Limestone	4.8	27.0
			27.0	36.0	Marl	27.0	57.0
8	BH- F	30.0	0.0	2.0	Clay	0.0	2.5
			2.0	5.1	Shale	2.5	5.4
			5.1	6.0	Marl		
			6.0	19.5	Limestone	5.4	19.5
			19.5	22.0	Marl	19.5	57.0
			22.0	23.5	Sand		
			23.5	30.0	Marl		

Fig. 5 Overburden isopach map

Overburden Isopach Map
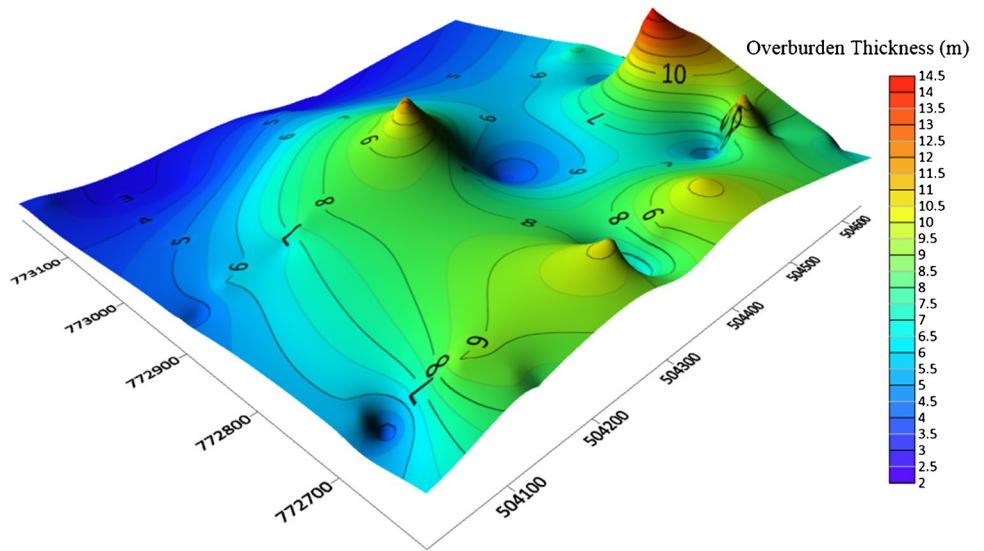
values of the overburden rock, and the limestone deposits were interpolated using the Surfer software to produce the isoresistivity, overburden, and limestone deposit isopach maps.

Results and discussion

The results of the 2D ERT survey along with the profiles are presented in Fig. 4. A critical observation of these models indicates that they are essentially similar in terms of their signatures except for the higher depth of investigation achieved with the pole-dipole array and a better lateral resolution with a dipole–dipole array. A maximum depth of investigation of 34.8 m was achieved by the dipole–dipole array, while a depth of 57 m was probed by the pole-dipole array. The observed electrical resistivity ranged from 1.0 to 13,000 Ωm, and it is the characteristic of varying conductivity and mineral composition in the subsurface. Available drill hole logs were used to constrain the interpretation of the 2D ERT sections, and strong positive correlation was established. (Table 1). Generally, four geoelectric stratums

Fig. 6 Isopach map of the limestone deposit
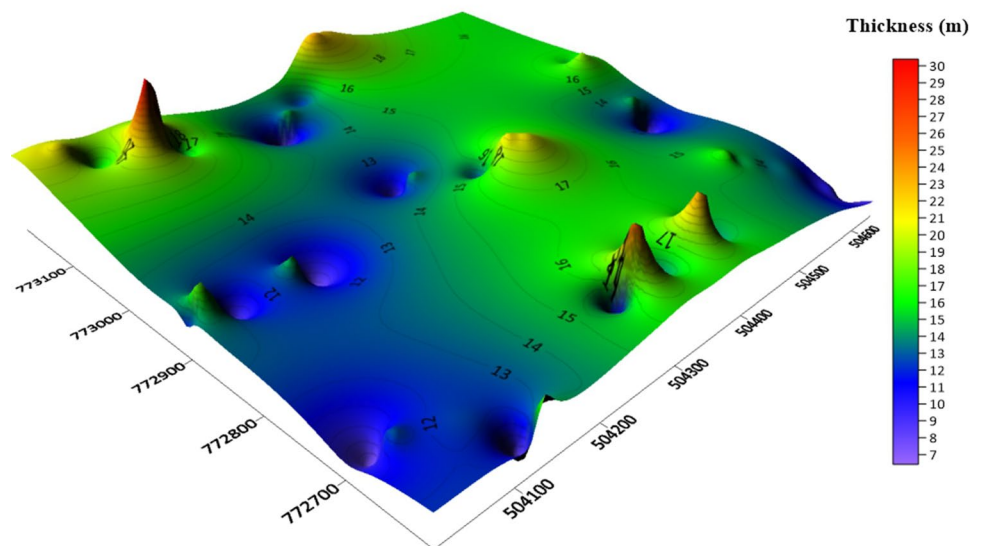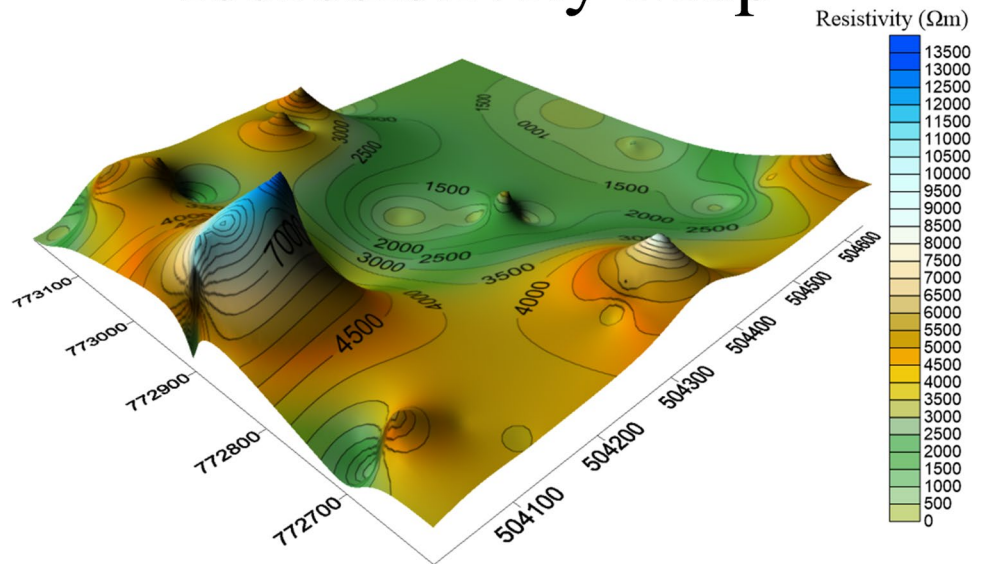
Isopach map of the limestone deposit

Isoresistivity Map

were delineated in all the 2D ERT sections except for traverse four which was characterized by three bands (Table 1). The low resistivity (1.0–50 Ωm) around the middle of some

of the profiles may be attributed to the possible dissolution of limestone, thus creating a cavity or void spaces within the rock. Physical observation shows that regions of cavitation
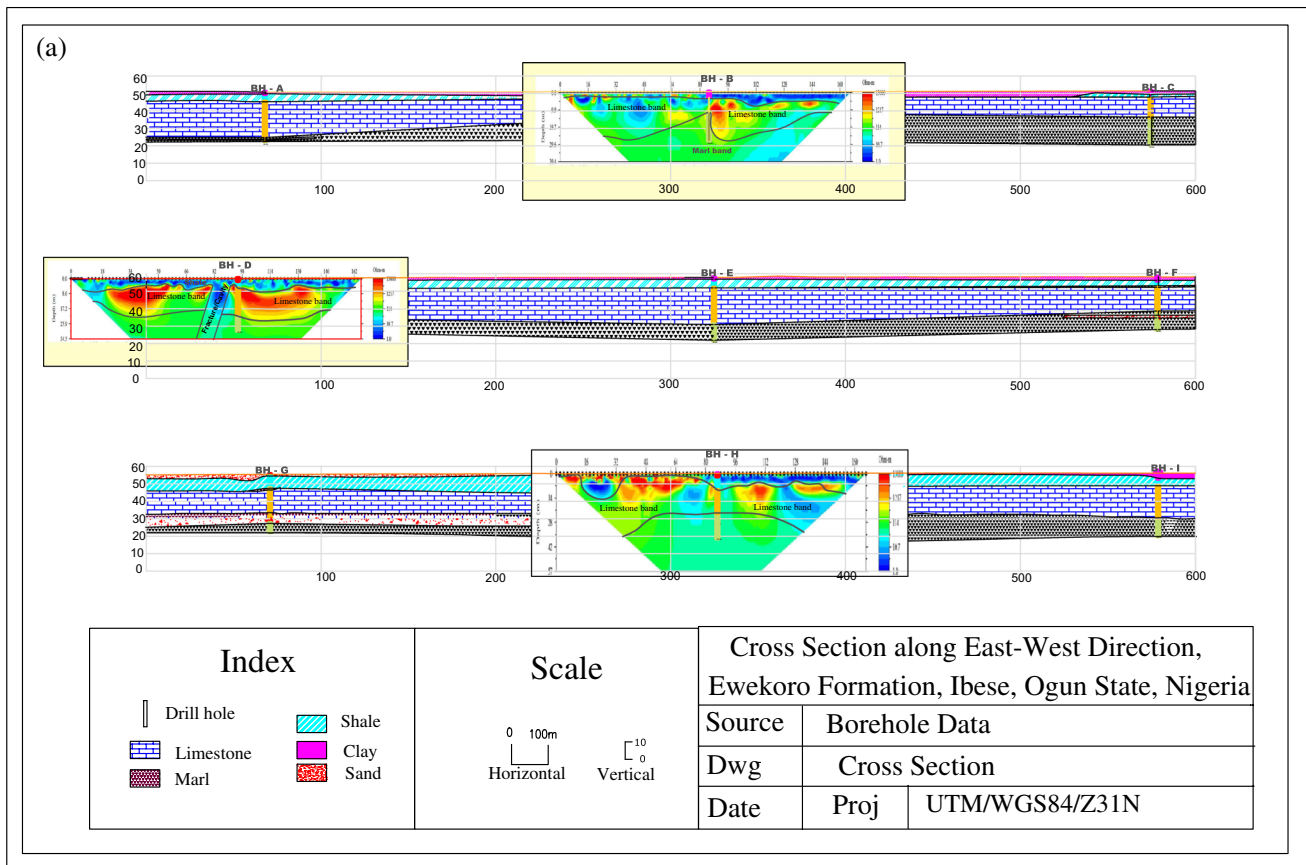

Fig. 8 **a** Cross-sectional view of boreholes along the East–West direction. **b** Cross sectional view of boreholes along the north-south direction
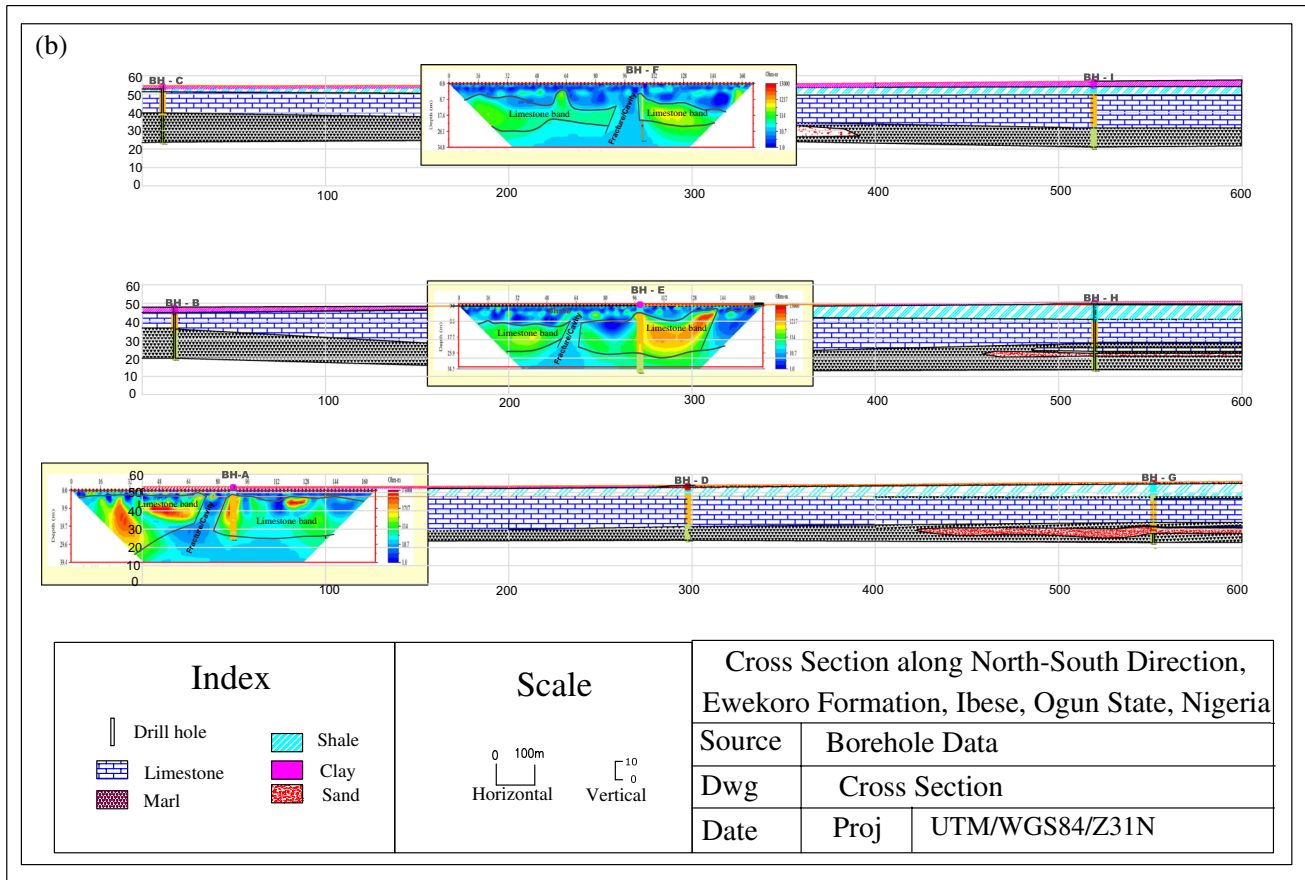
Fig. 8 (continued)

are impregnated with groundwater and may result in flooding during mining.

The orientation of the 2D models in Fig. 4a, b (traverse one) is towards the southeast-northwest direction, and four geoelectric layers/strata were delineated. The first layer is mostly clay having resistivity values around 1.0 to 100 Ωm occurring between 0 and 3 m in depth. The underlying stratum, interpreted as shale occurs at 3–16 m at the subsurface from about 64 m to the end of the traverse, and has resistivity ranging from 1.0 to 50 Ωm. The third layer occurs at depth of 4.0–28 m from the origin of the profile to about 112 m along the surface. It has resistivity values ranging from 200 to 13,000 Ωm and is interpreted as limestones. The fourth geoelectric layer is present at a depth of 26–57 m beneath the surface, with a resistivity of 100–400 Ωm. When correlated with borehole logs, it was deduced to be composed of marl.

The limestone is characterized by relatively high resistivity values at variable depths suggestive of a hard limestone bed, except for an important feature having low resistivity values between 64 and 85 m along the profiles indicating

limestone as well. This feature is interpreted as a cavity, and it extends from the shallow-weathered zones into the hard limestone and could have resulted from the weathering effects of surface and groundwater inside the limestone (Mohamed and Fouzan 2013).

Traverse three (Fig. 4c) has its orientation along the northwest-southeast direction. The first geoelectric layer here has resistivity values ranging from 1.0 to 1200 Ωm and occurs at a depth of 0–3 m. It is predominantly sand/topsoil. When correlated alongside the borehole log, the second geoelectric layer is found to have a depth of 1.0–7 m, with resistivity ranging from 1.0 to 80 Ωm. It is interpreted as shale/marl with some isolated high resistivity (1000–13,000 Ωm) due to the possible presence of limestone/intercalation of limestone. The third geoelectric component extends from a depth of 8.7–26.5 m, with a resistivity range from 200 to 13,000 Ωm. It is composed predominantly of limestone when tied to the lithology log. The fourth geoelectric stratum extends from 26 to 34.8 m, with resistivity ranging from 100 to 400 Ωm and suggestive of the presence of marl. Also conspicuous on the

2D-inverted section is the presence of low resistivity cavity structure at a lateral distance of 82–88 m.

The thicknesses of the overburden rock and limestone was determined at each data location using 2D sections and a lithology log. The overburden isopach map (Fig. 5) consists of the thickness of all the materials above the limestone. The map shows the overburden is thickest in the eastern part of the map with a value of 14. 5 m and thinnest in the north-ernmost region. The limestone isopach map (Fig. 6) shows that the limestone is thickest around the north-western and south-eastern parts of the map. The general thickness of lime-stone is between 5.9 and 31.45 m with 21 m on average, and it is thinnest at the southwestern and the central north-ern region where a noticeable structural depression trending north-eastern—south-western part of the survey area. The limestone resistivity values were also interpolated to produce the isoresistivity map presented in Fig. 7. The resistivity of limestone generally ranges from low to high, i.e., 80–13,000 Ωm. The limestone resistivity map shows that the limestone bed is predominantly characterized by a very high resistiv-ity value (2000–13,000 Ωm) with few exceptions. The low resistivity is indicative of shallow groundwater level, the presence of clayey material, increased porosity due to karst structures, and the presence of fluid-filled cavities/karst struc-tures. Figures 8a and 8b, demonstrate a lateral continuity of the limestone deposit and inverted 2D sections superimposed on lithologic section of the boreholes in the study region, correlate well and further suggest the presence of limestone of commercial relevance.

Conclusion

2D electrical resistivity imaging has been integrated with borehole information in Ibese mines to determine the ver-tical and the lateral extent of limestone deposits. The study area is predominantly characterized by four geologic units from the interpreted 2D ERT sections. The results of over-burden and limestone thicknesses, suggest an enormous limestone resource of economic interest mineable in an environmentally friendly manner using surface mining technique rather than the blasting method. However, the occurrence of low resistivity (1–50 Ωm) in some parts of the limestone beds may constitute geohazards during mining, as these may be cavities or fractured zones as a result of a possible dissolution of the limestone. The 2D geoelectric models show that the regions of cavitation are highly impregnated with groundwater and may result in flooding during mining. Further assessment/evaluation of these cavities is recommended, and precautionary meas-ures should be put in place to ensure safe operation within the mining site.

Declarations

References

AGI, (2003). Earth imager 2D resistivity inversion software, version 1.5.10. Advanced Geosciences, Inc, Austin, TX

Ameloko AA, Ayolabi EA (2020) Geophysical and hydrophysical evaluation of groundwater around the Igbenre-Ekotedo dump-site Ota, South West Nigeria, using correlation and regres-sion analysis. Arab J Geosci 13:896. https://doi.org/10.1007/s12517-020-05875-w

Ameloko AA, Ayolabi EA, Okezie U (2020) Modeling groundwater total dissolved solid from derived electromagnetic data using multiple linear regression analysis: a case study of groundwater contamination. Model Earth Syst Environ 6:1863–1875

Ammar AI, Kamal KA (2018) Resistivity method contribution in determining of fault zone and hydro-geophysical characteristics of carbonate aquifer, eastern desert, Egypt. J Appl Water Sci 8(1). https://doi.org/10.1007/s13201-017-0639-9

Ayolabi EA, Folorunso AF, Eleyinmi AF, Anuayah EO (2009) Applica-tions of 1D and 2D electrical resistivity methods to map aquifers in a complex geologic terrain of foursquare camp, Ajebo, South-western Nigeria. Pacific J Sci Technol 10(2):657–666

Felix BF, Yomi BG (2013) Geology and occurrences of limestone and marble in Nigeria. J Nat Sci Res 3(11):60–65

Gobashy MM, Metwally AM, Abdelazeem M, Soliman KS, Abdel-halim A (2021) Geophysical exploration of shallow groundwater aquifers in arid regions: a case study of Siwa Oasis Egypt. Nat Resour Res 30:3355–3384

Golian M, Rostami H, Ostad-Ali-Askari K (2020) Prediction of tun-nelling impact on flow rates of adjacent extraction water wells. Quarterly Journal of Engineering Geology and Hydrogeology. Geol Soc London UK 53(2):236. https://doi.org/10.1144/qjegh2019-055

Haile T, Atsbaha S (2014) Electrical resistivity tomography, VES and magnetic surveys for dam site characterization, Wukro, Northern Ethiopia. J African Earth Sci 97:67–77. https://doi.org/10.1016/j.jafrearsci.2014.03.023

Hussain Y, Uagoda R, Borges W, Nunes J, Hamza O, Condori C, Aslam K, Jie D, Cárdenas-Soto M (2020) The potential use of geophysical methods to identify cavities, sinkholes and pathways for water infiltration. J Water 12:2289. https://doi.org/10.3390/w12082289

Lara DG, Giovanni L (2019) Passive and active electric methods: new frontiers of application. In Innovation in Near-Surface Geophys-ics. Instrumentation, Application, and Data Processing Methods. Institute for Archaeological and Monumental Heritage, National Research Council, Prov.le Lecce-Monteroni, Lecce, Italy 1–21

Loke MH, Barker RD (1996) Rapid least-squares inversion of appar-ent resistivity pseudosection by quasi-Newton method. Geophys Prospect 44:131–152

Loke MH (2003) Rapid 2D resistivity & IP inversion using the least-squares method. Geotomo Software, Manual

Mohamed M, Fouzan A (2013) Application of 2-D geoelectrical resis-tivity tomography for subsurface cavity detection in the eastern part of Saudi Arabia. Geosci Front 4:469–476

Morrison, Gasperikova (2012) DC Resistivity and IP field systems, data processing and interpretation: California Berkeley, University of California Berkeley Department of Earth and Planetary Science

Obihan I, Ameloko AA, Kalejaiye FO, Ngozi-Chika CS, Rotimi OJ (2021) Evaluation of groundwater potential in part of Ahmadu Bello University Zaria Northwest Nigeria. SN Appl Sci. https://doi.org/10.1007/s42452-021-04210-6

Oluwaseun TO, Badmus BS, Akinyemi OD, Olowofela JA, Ozebo VC, Ganiyu SA (2012) Analysis of physical parameters of limestone deposits in Ewekoro Formation, Southwestern Nigeria. Earth Sci Res 1(2). https://doi.org/10.5539/esr.v1n2p117

Ozebo YE, Odunaike RK, Balogun AA (2008) Identification of depth to top of limestone body within a concession at Ibese, Southwestern Nigeria, using vertical electric sounding. Online J Earth Sci 2(3):99–107 (ISSN: 1991-7708)

Rita MC, Adedeji AA (2021) Assessment of heavy metals and microbial loads within the coal mines of Anambra basin, North Central, Nigeria. Journal of Global Ecology and Environment. 13(1), 22–35. https://www.ikprress.org/index.php/JOGEE/article/view/7037.

Serra R (2006) Dictionary of Geology. Academic (India) Publishers, New Delhi – 110008

Sum CW, Othman J, Loganathan P (1996). Geotechnical problems in limestone terrain with emphasis on cavities and sinkholes. Seminar Geologi dan Sekitarn, UKM, Puri Pujangga, Bangi, pp. 102e117